

Coherent feedback-enhanced asymmetry of thermal process in open quantum systems: Cavity optomechanics

Hamza Harraf,¹ Mohamed Amazioug,^{2,*} and Rachid Ahl Laamara^{1,3}

¹*LPHE-Modeling and Simulation, Faculty of Sciences, Mohammed V University in Rabat, Rabat, Morocco*

²*LPTHE-Department of Physics, Faculty of Sciences, Ibnou Zohr University, Agadir 80000, Morocco*

³*Centre of Physics and Mathematics, CPM, Faculty of Sciences, Mohammed V University in Rabat, Rabat, Morocco*

Entropy production is a fundamental concept in nonequilibrium thermodynamics, providing a direct measure of the irreversibility inherent in any physical process. In this work, we investigate in steady-state the enhancement of irreversibility employing coherent feedback loop. We evaluate the steady-state entropy production rate and quantum correlations by applying the quantum phase space formulation to calculate the entropy change. Our study reveals the essential contribution of coherent feedback in the thermal bath's input-noise operators, resulting in the system being driven far from thermal equilibrium. Our analysis shows that in the small-coupling limit, the entropy production rate is proportional to the quantum mutual information. We use for application the optomechanical system of Fabry-Pérot cavity, and show that the picks of the entropy production corresponding of the heating/cooling of movable mirror are improved. Therefore, we conclude that irreversibility and quantum correlations are not independent and must be analyzed jointly. The results demonstrate the possibility of enhancement of entropy production and pave the way for promising quantum thermal applications through coherent feedback loop.

I. INTRODUCTION

Entropy is considered as a fundamental measure that connects seemingly different notions like disorder, information, and irreversibility, playing a pivotal role in understanding dynamical processes [1, 2]. In the microscopic picture, the total entropy of a system in state ρ writes as

$$S(\rho) = -\text{tr}(\rho \log \rho). \quad (1)$$

Any transformation that occurs within a finite-time results in the production of entropy, signifying the irreversible nature of the process. The irreversible entropy generated by a process is of paramount importance. Entropy production leads for understanding nonequilibrium systems, and minimizing it can significantly enhance the efficiency of thermal machines. However, microscopic definition of entropy production is particularly challenging. Besides, entropy production is a fundamental quantity, its direct measurement remains elusive. This presents a significant challenge, especially when applying thermodynamic considerations. Furthermore, the emergence of correlations within a quantum system is intrinsically tied to the generation of entropy. This suggests that irreversibility and the formation of correlations are interconnected and cannot be considered independently. The entropy production rate, dictated by the second law of thermodynamics, must always be positive or zero [3, 4]. This yields the following rate equation for entropy change

$$\Delta S - \int \frac{\delta Q}{T} \geq 0, \quad (2)$$

where, T represents the temperature of the system, and δQ denotes the infinitesimal amount of heat absorbed by the system. The strict inequality indicates that irreversible processes are accompanied by energy dissipation, where some energy is lost to the environment as heat [5]. The rate of variation of entropy for a system interacting with a thermal bath is given by

$$\frac{dS}{dt} = \Phi(t) + \Pi(t), \quad (3)$$

in this equation, $\Pi(t)$ represents the irreversible entropy production rate, while $\Phi(t)$ represents the flux of entropy from the surrounding environment. Once the system reaches a stationary state, the irreversible entropy production rate becomes Π_s and the entropy flux becomes Φ_s . In this state, $\Pi_s = -\Phi_s > 0$. Only when both Π_s and Φ_s are zero, the system attains thermal equilibrium.

In the classical realm, entropy production is typically studied using Onsager's theory [6, 7], classical master equations [8], and Fokker-Planck equations [9, 10]. Extending these concepts to the quantum domain involves quantum master equations

*m.amazioug@uiz.ac.ma

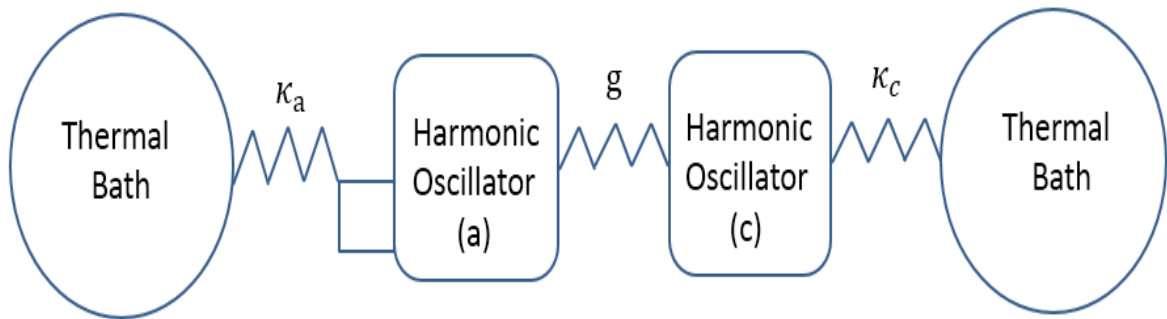


FIG. 1: Schematic of the system.

[11, 12]. Within this framework, entropy production can be quantified in terms of the mean values, variances, and irreversible quasi-probability currents in phase space. This approach has been applied to single-mode Gaussian systems coupled to a single reservoir [13–15] and multi-mode Gaussian systems interacting with multiple reservoirs [16, 17]. This underscores that the Wigner entropy production rate stays finite, even for a system coupled to a thermal reservoir at zero temperature [18]. The thermodynamic cost associated with establishing correlations between systems has been examined [19], adopting a purely information-theoretical approach without considering their dynamical origins. The generation of correlations and production of entropy are complementary aspects in a dissipative process [15]. Experimental results have shown good agreement with the theoretical predictions of this formalism [20].

Significant attention has recently been paid to coherent feedback in the fields of quantum information. Wiseman first discussed coherent feedback within the optical system [21, 22]. By using an asymmetric beam splitter to direct the input light field to the cavity, coherent feedback is achieved in a Fabry-Pérot cavity optomechanical setup. Moreover, a portion of the output electromagnetic field is reflected by the mirror and then fed back into the cavity through an asymmetric beam splitter. Feedback control is central to a wide range of applications, including the cooling of mechanical oscillators [23–25] and the entanglement of superconducting qubits [26]. Optomechanical systems [27, 28], trapped ions [29], cooling and trapping single atoms [30], trapped nanospheres [31, 32], and entanglement generation protocols [34–37] and quantum state transfer [38] are current platforms for coherent feedback implementation.

This paper investigates irreversibility in a bipartite quantum system with coherent feedback. A simplified model system consisting of two linearly interacting quantum oscillators, each dissipating into a local thermal bath, is studied. This system, despite its simplicity, captures many essential features of quantum-controlled experiments. The expression for the steady-state rate of irreversible entropy production is utilized [15]. This expression links irreversibility to either the number of excitations in the two modes (relative to their equilibrium values) or the correlations between their motion. This clarifies how irreversibility emerges. We prove the enhancement of non-equilibrium between the two oscillators via coherent feedback. We compare the behavior of entropy production with total correlations, which are quantified by mutual information [39, 40]. We observe that entropy production exhibits a monotonic relationship with mutual information. We find a simple proportionality between entropy production and mutual information, specifically when the coupling between the systems is weak compared to their natural frequencies. We utilize our results for the quantification of irreversibility in an optomechanical system [41]. Besides, system characteristics influence the behavior of entropy production in various regimes, such as cavity-mediated cooling and amplification of the mechanical resonator.

The remainder of this paper is outlined as follows: In Section II, we suggest the model and quantum Langevin equations of motion of coupled quantum oscillators. In Section III, we discuss the covariance matrix of the system, the stationary entropy production rate, and quantum correlation quantified by mutual information and negativity logarithmic. In Section IV, is devoted to discussion of the results. In Section V, we consider an optomechanical system as an application of the system under consideration. The conclusion is presented in Section VI.

II. THE MODEL OF COUPLED QUANTUM OSCILLATORS

The system under consideration comprises two coupled harmonic quantum oscillators, each dissipating into its own local thermal bath, as depicted in Fig. 1. The Hamiltonian of the interacting system is described by

$$\mathcal{H} = \Omega_{\text{fb}} \hat{a}^\dagger \hat{a} + \Omega_c \hat{c}^\dagger \hat{c} - g(\hat{a} + \hat{a}^\dagger)(\hat{c} + \hat{c}^\dagger), \quad (4)$$

where the two harmonic oscillators have annihilation (creation) operators $\hat{a}(\hat{a}^\dagger)$ and $\hat{c}(\hat{c}^\dagger)$, and frequencies Ω_{fb} and Ω_c , respectively. Equation (4) describes the system's Hamiltonian, where the first two terms represent the free energies of the harmonic oscillators and the last term denotes their coupling with coupling constant g . Each of the two harmonic oscillators dissipates into its local thermal bath (bath 1 at rate κ_a , bath 2 at rate κ_c). Assuming the baths are mutually independent, the system is also subjected to additional quantum noise, described by the input operators a^{in} ; c^{in} satisfying Markovian correlation functions

$$\langle \hat{a}_{\text{fb}}^{in}(t) \hat{a}_{\text{fb}}^{in\dagger}(t') \rangle = \xi^2 |1 - \tau e^{i\theta}|^2 (N_a + 1) \delta(t - t'), \quad (5a)$$

$$\langle \hat{a}_{\text{fb}}^{in\dagger}(t) \hat{a}_{\text{fb}}^{in}(t') \rangle = \xi^2 |1 - \tau e^{i\theta}|^2 N_a \delta(t - t'), \quad (5b)$$

$$\langle \hat{c}^{in}(t) \hat{c}^{in\dagger}(t') \rangle = \langle \hat{c}_{in}^\dagger(t) \hat{c}_{in}^\dagger(t') \rangle = 0, \quad (5c)$$

$$\langle \hat{c}^{in}(t) \hat{c}^{in\dagger}(t') \rangle = (N_c + 1) \delta(t - t'), \quad (5d)$$

where the thermal occupation number associated with reservoir i (at temperature T_i , for $i = a, c$) is given by

$$N_a = (e^{\hbar\Omega_a/k_B T_a} - 1)^{-1}, \quad N_c = (e^{\hbar\Omega_c/k_B T_c} - 1)^{-1}, \quad (6)$$

where k_B is the Boltzmann constant. The beam splitter has a real amplitude transmission parameter ξ and a real amplitude reflectivity parameter τ . These real, positive quantities satisfy $\xi^2 + \tau^2 = 1$. Incorporating dissipation from system-bath couplings and their corresponding noises, the quantum Langevin equations of motion are given by

$$\begin{aligned} \dot{\hat{a}} &= -(i\Omega_{\text{fb}} + \kappa_{\text{fb}})\hat{a} + ig(\hat{c} + \hat{c}^\dagger) + \sqrt{2\kappa}a_{\text{fb}}^{in}, \\ \dot{\hat{c}} &= -(i\Omega_c + \kappa_c)\hat{c} + ig(\hat{a} + \hat{a}^\dagger) + \sqrt{2\gamma}c^{in}, \end{aligned} \quad (7)$$

the effective cavity decay rate and detuning are given by $\kappa_{\text{fb}} = \kappa_a(1 - 2\tau \cos \theta)$ and $\Omega_{\text{fb}} = \Omega_a - 2\kappa_a \tau \sin \theta$, respectively. In these expressions, θ represents the phase shift generated by the reflectivity of the output field on the mirrors. The standard input-output relation relating the output field \hat{a}^{out} and the cavity field \hat{a} is $\hat{a}^{\text{out}} = \sqrt{2\kappa_a}\hat{a} - a^{in}$ [33]. To describe the input field induced via the coherent feedback, we introduce the effective input noise operator \hat{a}_{fb}^{in} , given by $\hat{a}_{\text{fb}}^{in} = \tau e^{i\theta} \hat{a}^{in} + \tau \hat{a}^{in}$.

III. ENTROPY PRODUCTION RATE AND QUANTUM MUTUAL INFORMATION

We define the EPR-type quadrature operators for the two modes as $\hat{X}_a = (\hat{a} + \hat{a}^\dagger)/\sqrt{2}$, $\hat{Y}_a = (\hat{a} - \hat{a}^\dagger)/i\sqrt{2}$, $\hat{X}_c = (\hat{c} + \hat{c}^\dagger)/\sqrt{2}$ and $\hat{Y}_c = (\hat{c} - \hat{c}^\dagger)/i\sqrt{2}$ (and their corresponding input noise quadratures). With the coupling strength $\mathcal{G} = 2g$, this allows the quantum Langevin equations for the quadratures to be written in a compact matrix form

$$\dot{\hat{u}}(t) = \mathcal{A}\hat{u}(t) + \eta(t), \quad (8)$$

where $\hat{u}(t) = \{\hat{X}_a, \hat{Y}_a, \hat{X}_c, \hat{Y}_c\}^T$ and $\eta(t) = \{\sqrt{2\kappa_{\text{fb}}}\hat{X}_a^{in}, \sqrt{2\kappa_{\text{fb}}}\hat{Y}_a^{in}, \sqrt{2\kappa_c}\hat{X}_c^{in}, \sqrt{2\kappa_c}\hat{Y}_c^{in}\}^T$ are, respectively, the vector of operators and the vector of noises. The drift matrix \mathcal{A} is given by

$$\mathcal{A} = \begin{bmatrix} -\kappa_{\text{fb}} & \Omega_{\text{fb}} & 0 & 0 \\ -\Omega_{\text{fb}} & -\kappa_{\text{fb}} & \mathcal{G} & 0 \\ 0 & 0 & -\kappa_c & \Omega_c \\ \mathcal{G} & 0 & -\Omega_c & -\kappa_c \end{bmatrix}, \quad (9)$$

if all eigenvalues of the drift matrix \mathcal{A} have negative real parts, the system is stable and reaches a steady-state. The linear dynamics and Gaussian quantum noise terms lead to the system reaching a continuous variable (CV) Gaussian steady-state. This state can be characterized by the 4×4 covariance matrix (CM) \mathcal{V} , whose components are given by

$$\mathcal{V}_{ij} = \langle \hat{u}_i(\infty) \hat{u}_j(\infty) + \hat{u}_j(\infty) \hat{u}_i(\infty) \rangle / 2. \quad (10)$$

Given that the first moments are zero, covariance matrix (CM) are constrained by the uncertainty relations among canonical operators ($[\hat{u}_i, \hat{u}_j] = i\Omega_{ij}$). This imposes the inequality $\mathcal{V} + i\Omega/2 \succeq 0$, where Ω is the symplectic matrix [46]. The Lyapunov equation characterizes the steady state of the system, and is expressed as

$$\mathcal{A}\mathcal{V} + \mathcal{V}\mathcal{A}^T = -\mathcal{D}, \quad (11)$$

where $\mathcal{D} = \text{diag}\{K_a(2N_a+1), K_a(2N_a+1), \kappa_c(2N_c+1), \kappa_c(2N_c+1)\}$ is the diffusion matrix, with $K_a = \kappa_a(1-\tau^2)|1-\tau e^{i\theta}|^2$. While Equation (11) is readily solvable, its full analytical expression is too cumbersome to be presented here. The steady-state entropy production rate (Π_s) and entropy flux rate (ϕ_s) are determined to be as presented in the Appendix [47–49]

$$\begin{aligned} \Pi_s = -\phi_s &= \text{Tr}[\mathcal{A}^{irr} + 2\mathcal{A}^{irr}\mathcal{D}^{-1}\mathcal{A}^{irr}\mathcal{V}^s] \\ &= 2\kappa_{fb} \left[\frac{\kappa_{fb}}{K_a} \frac{(\mathcal{V}_{11}^s + \mathcal{V}_{22}^s)}{(2N_a+1)} - 1 \right] + 2\kappa_c \left[\frac{\mathcal{V}_{33}^s + \mathcal{V}_{44}^s}{2N_c+1} - 1 \right] \\ &= \mu_a + \mu_c, \end{aligned} \quad (12)$$

where $\mathcal{A}^{irr} = \text{diag}\{-\kappa_{fb}, -\kappa_{fb}, -\kappa_c, -\kappa_c\}$. When the system is in the equilibrium state: $\mathcal{V}_{11}^s + \mathcal{V}_{22}^s = \frac{K_a}{\kappa_{fb}}(2N_a+1)$ and $\mathcal{V}_{33}^s + \mathcal{V}_{44}^s = 2N_c+1$, and hence, $\Pi_s = 0$ [49–51]. We define the first term as contribution a to the entropy production rate (μ_a), as it depends solely on quantities labeled by a. Analogously, the second term, dependent on quantities labeled by c, is defined as contribution c (μ_c)

$$\mu_k = 2\kappa_k \left(\frac{N_{k,s} + 1/2}{N_k + 1/2} - 1 \right), \quad (k = a, c), \quad (13)$$

the terms $N_{a,s}$ and N_a represent $\langle \hat{a}^\dagger \hat{a} \rangle_s$ and $\langle \hat{a}^\dagger \hat{a} \rangle_{\text{eq}}$, respectively, with μ_c defined similarly. Equation (13) links the irreversibility generated by the stationary process to the change in each oscillator's excitation level from its equilibrium value. For a noninteracting system, where each oscillator equilibrates with its individual bath, Π_s identically vanishes, as demonstrated by Eq. (13).

Mutual information, defined as $\mathcal{I}(\varrho_{a:c}) = S(\varrho_a) + S(\varrho_c) - S(\varrho_{ac})$, quantifies the total correlations shared between two systems [52], using the von Neumann entropy for Gaussian distributions

$$S(\mathcal{V}_{ac}) = \frac{1}{2} \log(\det \mathcal{V}_{ac}). \quad (14)$$

According to Ref. [53], $S(\mathcal{V}_{ac})$ coincides (up to an additive constant) with the generalized Rényi entropy of order 2 ($S_2(\varrho) = -\log \text{tr} \varrho^2$). Mutual information is defined as $\mathcal{I}(\mathcal{V}_{a:c}) = S(\mathcal{V}_{ac}) - S(\mathcal{V}_a) - S(\mathcal{V}_c)$. Moreover, Eq. (14) implies that

$$\mathcal{I}(\mathcal{V}_{a:c}) = -\frac{1}{2} \log \left(\frac{\det \mathcal{V}}{\det \mathcal{V}_a \det \mathcal{V}_c} \right). \quad (15)$$

We quantify bipartite entanglement using the logarithmic negativity E_N [56–58], which takes the form

$$E_N = \max[0, -\log(2\nu^-)], \quad (16)$$

where, ν^- is the minimum symplectic eigenvalue of the covariance matrix \mathcal{V} :

$$\nu^- = \frac{1}{\sqrt{2}} \sqrt{\mathcal{L} - (\mathcal{L}^2 - 4\det \mathcal{V})^{1/2}},$$

with $\mathcal{L} = \det \mathcal{V}_a + \det \mathcal{V}_c - 2\det \mathcal{V}_{ac}$. The condition $\nu^- < 1/2$ is the necessary and sufficient criterion for entanglement between the two modes, as it directly corresponds to a positive logarithmic negativity ($E_N = -\log(2\nu^-) > 0$).

IV. RESULTATS AND DISCUSSION

In this section we will show the importance technique of coherent feedback, that enable one to generate the irreversibility in the equilibrium ($N_a = N_c = 0$), and also its importance to enhances the irreversibility entropy production. We plot the stationary entropy production rate Π_s and its constituent components μ_a and μ_c in Fig. 2 where the reservoirs are in the ground state $N_a = N_c = 0$ in panels (a)-(c), versus the frequency ω_a with solid black curves in the plots correspond to identical loss rates $\kappa_{fb} = \kappa_c$ conversely, the solid red curves are for $\kappa_a = 0.2$, $\kappa_c = 0.5$. In Fig. 2, Π_s , μ_a and μ_c are increased via $\tau = 0.9$. This is compared with the results discussed in Ref. [42].

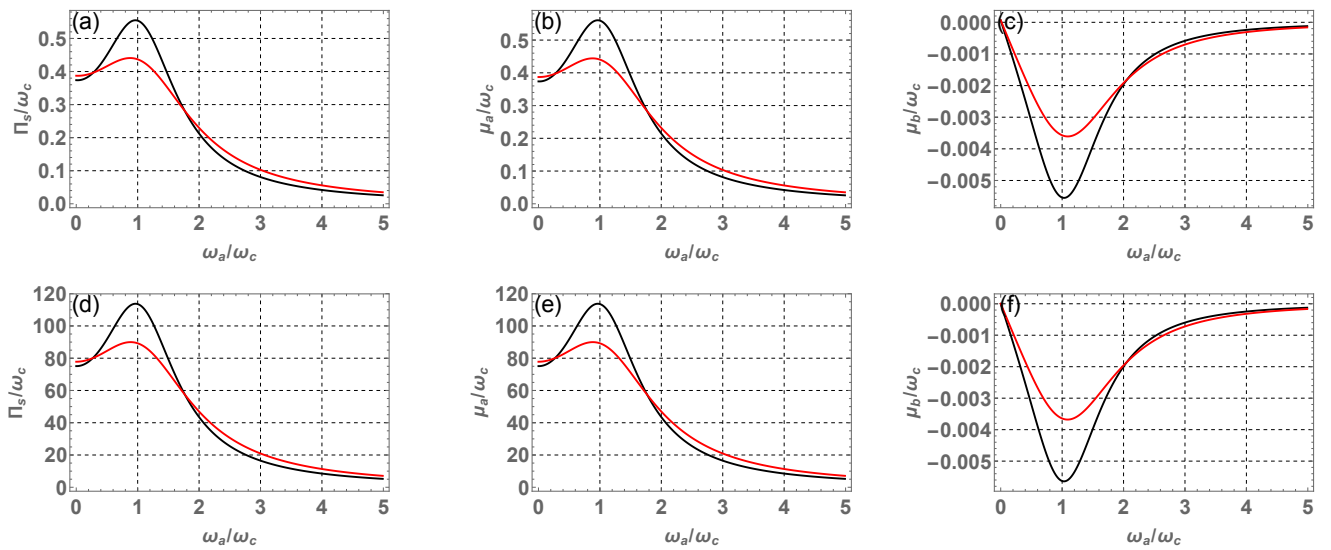


FIG. 2: Entropy production rate Π_s/ω_c and its two contributions μ_a/ω_c and μ_c/ω_c against the ratio of the two frequencies for different values of κ_c with $\kappa_a = \kappa_c = 0.2\omega_c$ correspond to the Back curves, while $\kappa_a = 0.2\omega_c$ and $\kappa_c = 0.5\omega_c$ correspond to the Red curves. In panels (a), (b), (c) when the reservoirs occupy their ground state $N_a = N_c = 0$. In panels (d), (e), (f) an imbalance in thermal excitations is considered, where $N_a = 0$ and $N_c = 100$. We use parameters are $G = 0.1\omega_c$ $\tau = 0.9$ and $\theta = \pi$.

Moreover, in panels (a)-(c), we remark that μ_a is positive, while μ_c displays a negative dip. However, one can explain the change of sign of μ_c from positive ($\tau = 0$) to negative ($\tau = 0.9$) by coherent feedback ($\tau = 0.9$), i.e., μ_a and μ_c are not similar in the ground state. Furthermore, Fig. 2 shows Π_s approaching zero for $\omega_a \gg 1$. When the oscillators are far off resonance, they effectively decouple, leading to each thermalizing with its own bath. The notable disparity in magnitude between μ_a and μ_c leads to the overall positivity of Π_s .

This can be explained by the emergence of an imbalance in thermal excitation's by increasing the initial thermal occupation of the oscillators with respect to their initial value, through the *coherent feedback loop that re-injects photons into the cavity*. Furthermore, consistent with Eq. (13), a steady negative value of μ_c indicates a reduction in steady excitations ($N_{c,s} < N_c$) and thus an effective cooling of oscillator c , and increases of steady excitations $N_{a,s} > N_a$ and thus an effective heating of oscillator a . This directly results from the enforced asymmetry between the two subsystems, a characteristic observable even if $N_a = N_c = 0$. We observe that $\Pi_s \approx \mu_a$, featuring a distinctive peak at $\omega_a = \omega_c$. Moreover, at $\omega_a = \omega_c$, we see that Π_s , μ_a and $|\mu_c|$ achieve its maximum value for equal loss $\kappa_a = \kappa_c$. It is also evident from Fig. 2(a)-(c) that Π_s generally broadens with increasing losses, κ_a and κ_c .

If we consider initial thermal occupation in one oscillator, specifically $N_c = 100 > 0$ as shown in Fig. 2(d)-(f), Π_s is found to approximate μ_a and displays a distinctive peak at $\omega_a = 1$. In parallel, μ_c exhibits a negative dip. This figure show also that coherent feedback lead to enhance the degree of irreversibility, in comparison with the results shown in Ref. [42]. A comparison of panels (a) and (d) immediately reveals that employing a coherent feedback loop (under conditions where $N_a = N_c = 0$) or can be made to grow by introducing an imbalance in the initial oscillator populations Π_s . This indicates irreversibility arising from transport, as the coupled oscillators now facilitate a net heat flux between the two baths. Consistent with Eq. (13), the observation of a steady negative μ_c value signifies a reduction in steady excitations $N_{c,s} < N_c$ and thus an effective cooling of oscillator a .

The peaks in μ_a and corresponding dips in μ_c at $\omega_a = 1$ (i.e., when the oscillators share identical frequencies). For $\omega_a \approx 1$ and $G < \omega_a$, adopting the rotating frame and applying the rotating-wave approximation yields an interaction Hamiltonian of the form $H_I \propto \hat{a}^\dagger \hat{c} + \hat{a} \hat{c}^\dagger$. The large degree of irreversibility can thus be attributed to the latter being a pure exchange interaction, rendering it optimal for heat transfer [43].

From Fig. 3, two distinct behaviors of Π_s are evident: it achieves its minimum at $N_a = N_c$, while for $N_c > N_a$, Π_s grows linearly with N_c , hence proportionally to the population imbalance. Within the regime where $N_c/N_a < 1$, we observe a sharp increase in the entropy production rate. This rate, however, consistently remains finite, including the case where $N_c = 0$. Also, we observe the enhancement of Π_s , μ_a and μ_c via coherent feedback loop. This in comprising with the results realized in Ref. [42]. Moreover, we see that Π_s increases with increasing G . This can be explained by the relationship between μ_k ($k = a, c$) and G . Furthermore, for $\tau = 0.1$ the μ_a remains positive, even if $N_a \ll N_c$. Moreover, μ_c is negative, around $N_a \geq N_c$, as also discussed in Ref. [42]. Besides, for $\tau = 0.1$ the Π_s remains > 0.1 . This dictates that Π_s will be reduced by the oscillator c and compensate by the oscillator a . In the small coupling regime, μ_a and μ_c effectively swap their dependencies on the thermal excitations N_a and N_c . The clear influence of the imbalance between N_a and N_c on μ_a and μ_c is evident from this figure,

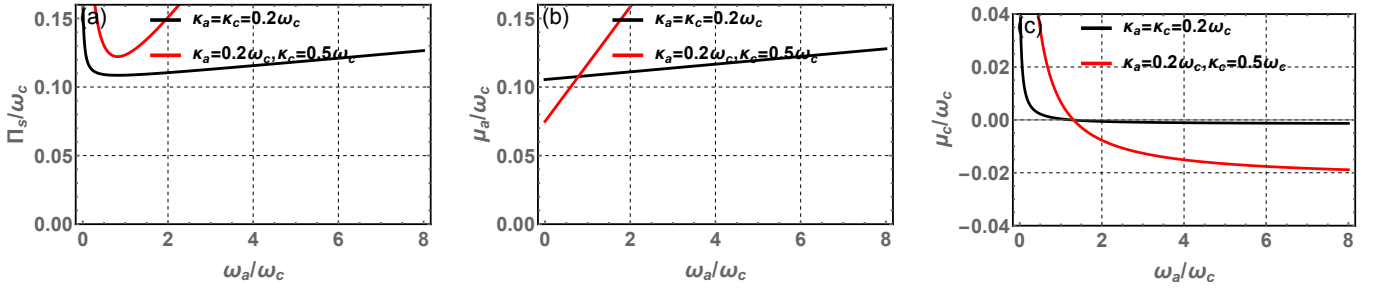


FIG. 3: Entropy production rate Π_s/ω_c (a) and its two contributions μ_a/ω_c (b) and μ_c/ω_c (c) against the ratio N_a/N_c for various value of G with $G = 0.05\omega_c$ correspond to the Back curves, while $G = 0.2\omega_c$ correspond to the Red curves. The oscillators have the same frequency $\omega_a = \omega_c$, $\kappa_a = 0.2\omega_c$ and $\kappa_c = 0.5\omega_c$, with $\tau = 0.1$ and $\theta = \pi$.

consequently determining which oscillator experiences local entropy reduction and which performs compensation.

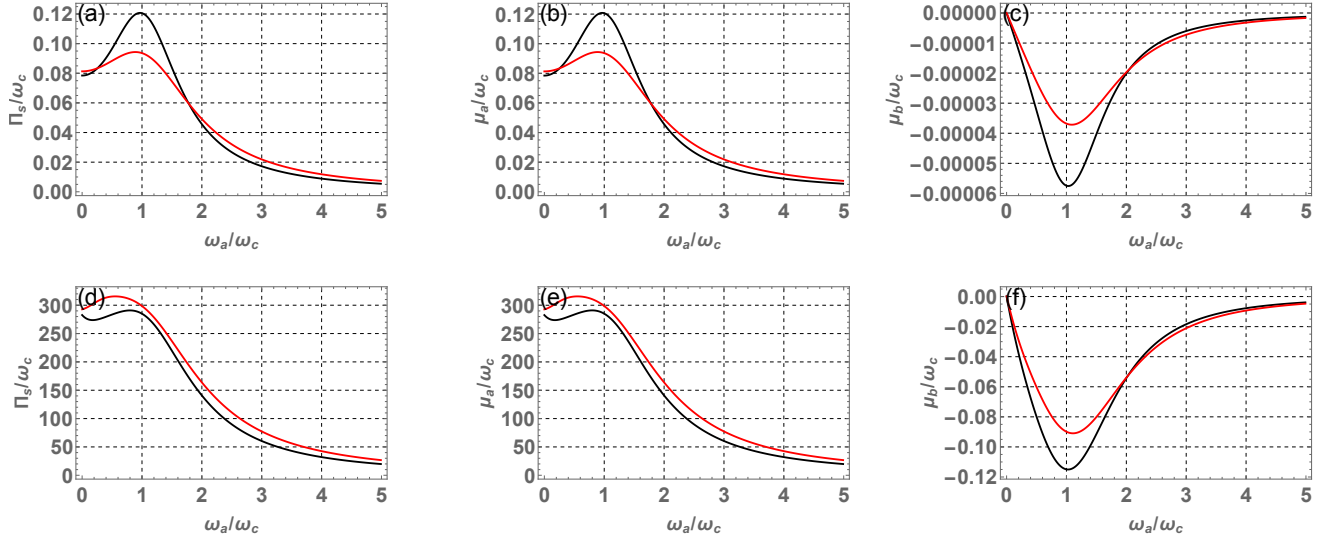


FIG. 4: Entropy production rate Π_s/ω_c and its two contributions μ_a/ω_c and μ_c/ω_c against the ratio of the two frequencies for different values of κ_c with $\kappa_a = \kappa_c = 0.2\omega_c$ correspond to the Back curves, while $\kappa_a = 0.2\omega_c$ and $\kappa_c = 0.5\omega_c$ correspond to the Red curves. In panels (a)-(c) we use $G = 10^{-2}\omega_c$ but in panels (d)-(f) we use $G = 0.6\omega_c$. Other parameters are $N_a = 0$ and $N_c = 10$, $\tau = 0.9$ and $\theta = \pi$.

We explore entropy production rate Π_s/ω_c and its two contributions μ_a/ω_c and μ_c/ω_c , as in Fig. 2 with $N_a = 0$ and $N_c = 10$, when coherent feedback is applied. While Fig. 4(a)-(c) ($G = 10^{-2}\omega_c$) and Fig. 4(d)-(f) ($G = 0.6\omega_c$) show Π_s/ω_c having the same shape, a striking difference is its magnitude, which decreases by two orders. In Fig. 4 (d)-(f), we observe that the Π_s/ω_c for $\kappa_a = \kappa_c = 0.2\omega_c$ is bounded by the one of $\kappa_a = 0.2\omega_c$ and $\kappa_c = 0.5\omega_c$. For $\tau = 0.9$, we remark the enhancement of irreversibility entropy production Π_s/ω_c and its two contributions μ_a/ω_c and μ_c/ω_c with increasing G , with respect to the results discussed in Ref. [42]. Additionally, Π_s shows a second peak around $\omega_a/\omega_c = 1$, consistent with hybridization effects.

We present in Fig. 5(a-f) the evolution of entropy production Π_s/ω_c and its components μ_a/ω_c and μ_c/ω_c versus the reflectivity parameter τ for various values of $\kappa_{a(c)}$ and $N_{a(c)}$. We notice the enhancement of Π_s/ω_c , μ_a/ω_c and μ_c/ω_c by increasing τ . Moreover, the coherent feedback contribute on a steady negative value of μ_c , i.e., an effective cooling of oscillator c , and on an effective heating of oscillator a , because μ_a increases. Also, an imbalance in thermal excitation's increases the entropy production. However, the entropy production Π_s/ω_c increase for $\kappa_a = \kappa_c = 0.2\omega_c$.

The striking similarity between Π_s and \mathcal{I} , shown in Fig. 6(a), (b), (d) and (e), reveals that \mathcal{I} is a one-to-one function of Π_s , despite their different functional forms. This result provides the first indication that the irreversibility arising from the

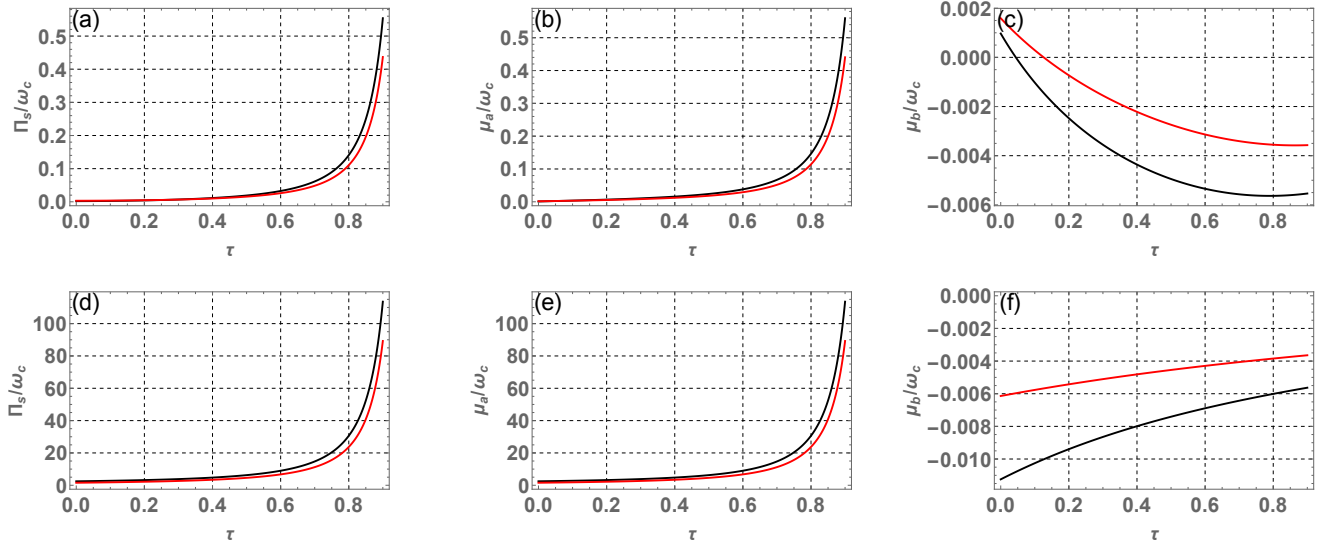


FIG. 5: Entropy production rate Π_s/ω_c and its two contributions μ_a/ω_c and μ_b/ω_c against the reflectivity parameter τ for various value of κ_c with $\kappa_a = \kappa_c = 0.2\omega_c$ correspond to the Back curves, while $\kappa_a = 0.2\omega_c$ and $\kappa_c = 0.5\omega_c$ correspond to the Red curves. In panels (a), (b), (c) the reservoirs are in the ground state $N_a = N_c = 0$, while in panels (d), (e), (f) we considering an imbalance in thermal excitations $N_a = 0$ and $N_c = 100$, with $\theta = \pi$ and $G = 0.1\omega_c$.

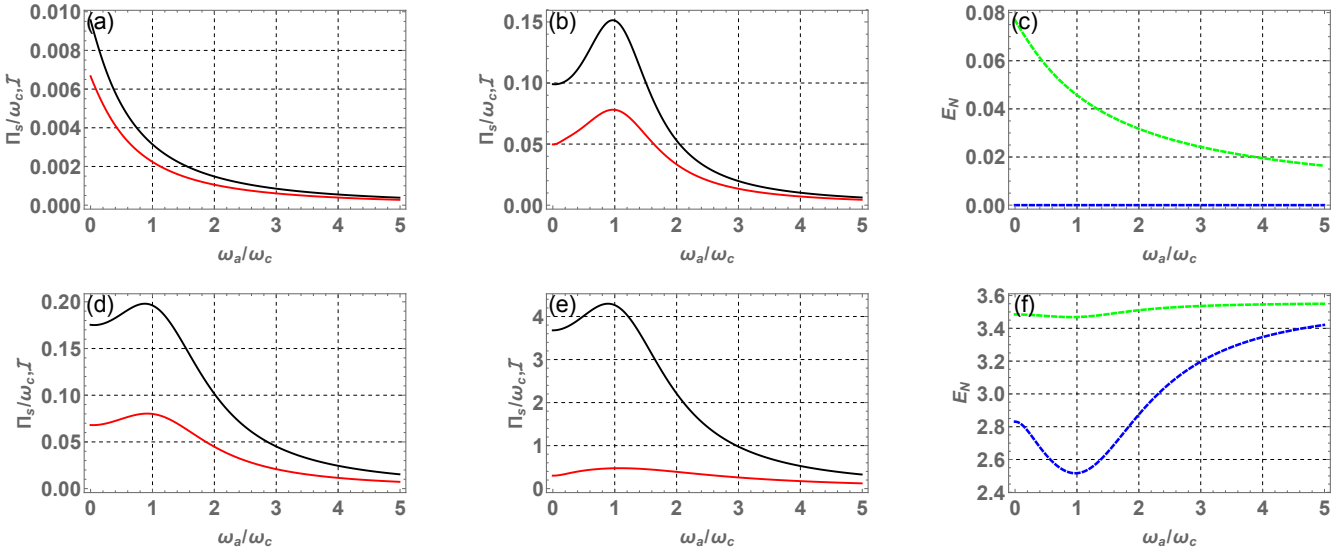


FIG. 6: Comparison of the steady-state entropy production rate Π_s/ω_c (Black curves), the mutual information \mathcal{I} (Red curves) and entanglement (Green and Blue curves) versus the ratio of the two frequencies ω_a/ω_c with $G = 0.1\omega_c$. In Panels (a), (d), (c) and (f) (Green and Blue curve) corresponds to $N_a = N_c = 0$, while in panels (b), (e), (c) and (f) (Blue curve) corresponds to $N_a = 0, N_c = 10$. With $\tau = 0$ in Panels (a), (d), (c) and $\tau = 0.85$ in Panels (b), (e), (f). With $\theta = \pi$.

stationary process is closely linked to the total correlations shared between the two modes. Decoupled oscillators (uncoupled or far-off-resonance) reach separate thermal equilibrium, leading to vanishing Π_s and \mathcal{I} . It can clearly be seen that in the presence of coherent feedback ($\tau = 0.85$), Π_s , \mathcal{I} and entanglement enhance. Besides, the increases of τ leads to enhancement of the region around the resonance, i.e., the two oscillators go far of equilibrium. Furthermore, panels (d) and (e) illustrate the enhancement of both Π_s and \mathcal{I} relative to the results shown in panels (a) and (b), respectively. In panel (c), the entanglement is vanishing for $N_a = 0, N_c = 10$. However, E_N is positive for $N_a = N_c = 0$. This means that the entanglement is fragile under thermal effect than both Π_s and \mathcal{I} . It can be seen that when $\tau = 0.86$, the entanglement is generated by coherent feedback when $N_a = 0, N_c = 10$.

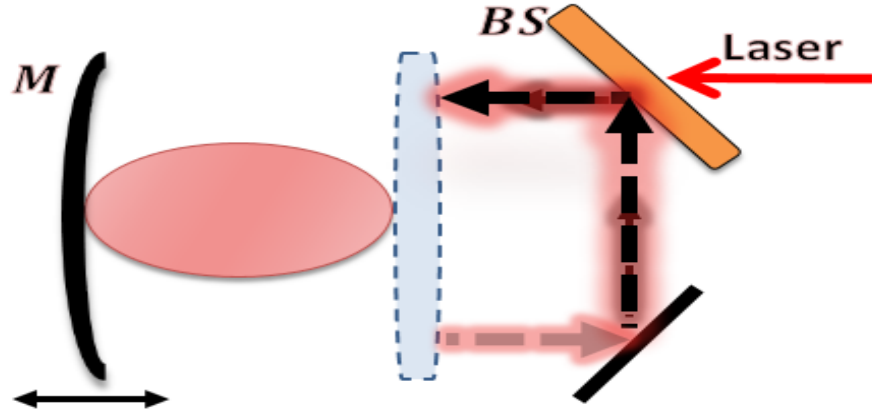


FIG. 7: Schematic of Fabry-Pérot cavity with coherent feedback. An input laser is coupled into the cavity through an asymmetric beam splitter (BS), which also routes a portion of the cavity's output field back into the cavity via a reflecting mirror.

V. APPLICATION : CAVITY OPTOMECHANICS

Characterization of the irreversibility in a cavity optomechanical system is performed in this section, utilizing our previously established results. Configured as a single-mode Fabry-Pérot cavity, this system includes a perfectly reflecting movable mirror (Fig. 7). Pumping the length- L cavity through the fixed mirror is a monochromatic laser field, characterized by frequency ω_0 and strength $E = \sqrt{\frac{2P\kappa_a}{\hbar\omega_0}}$ (P = laser power, κ = cavity decay rate). The optomechanical coupling between the cavity and the mechanical oscillator, with frequency ω_m , is enabled by the radiation pressure. In the rotating frame of the external pump, the system's Hamiltonian ($\hbar = 1$) is given by

$$H = \hbar\Delta_0\hat{a}^\dagger\hat{a} + \hbar\omega_m\hat{c}^\dagger\hat{c} - \hbar g_0\hat{a}^\dagger\hat{a}(\hat{c}^\dagger + \hat{c}) + i\hbar E\xi(\hat{a}^\dagger - \hat{a}), \quad (17)$$

The first two terms in the Hamiltonian H describe the energies of the individual cavity field and mechanical mode. Let $\Delta_0 = \omega_a - \omega_0$ be the cavity detuning, and g_0 be the single-photon optomechanical coupling strength, which quantifies the interaction between the cavity and the mechanical oscillator. The Hamiltonian's third term captures the radiation-pressure interaction, while the final term depicts the cavity driving in the presence of coherent feedback. For the beam splitter, ξ represents the real amplitude transmission parameter and τ the real amplitude reflectivity parameter. Both are real, positive, and satisfy $\xi^2 + \tau^2 = 1$ [59]. When coherent feedback of the cavity output is absent, the parameters are $\tau = 0$ and $\xi = 1$. We can obtain the following nonlinear quantum Langevin equations through the inclusion of dissipation arising from system-bath interactions. By including dissipation arising from system-bath interactions, we obtain the following nonlinear quantum Langevin equations

$$\dot{\hat{a}} = -(i\Delta_{fb} + \kappa_{fb})\hat{a} + ig\hat{a}(\hat{c} + \hat{c}^\dagger) + E + \sqrt{2\kappa}a_{fb}^{in}, \quad (18a)$$

$$\dot{\hat{c}} = -(i\omega_c + \gamma_c)\hat{c} + ig\hat{a}\hat{a}^\dagger + \sqrt{2\gamma}c^{in}, \quad (18b)$$

a_{fb}^{in} and c^{in} are input-noise operators, γ_c is the mechanical oscillator damping rate, and κ_{fb} is the cavity-field damping rate via feedback. When the driving laser amplitude is strong, both modes exhibit large steady-state amplitudes. We express each operator as the sum of its steady-state mean and a fluctuation: $\hat{a} = \hat{a}_s + \delta\hat{a}$ and $\hat{c} = \hat{c}_s + \delta\hat{c}$. The steady-state mean values are expressed as

$$\hat{a}_s = \frac{E}{i\Delta'_{fb} + \kappa_{fb}}, \quad \hat{c}_s = \frac{ig_0|\hat{a}_s|^2}{i\omega_c + \gamma_c},$$

where $\Delta'_{fb} = \Delta_{fb} - g_0(\hat{c}_s + \hat{c}_s^*)$ defines the effective cavity detuning. The linearized quantum Langevin equations governing the fluctuation operators are

$$\dot{\delta\hat{a}} = -(i\Delta_{fb} + \kappa_{fb})\delta\hat{a} + ig(\delta\hat{c} + \delta\hat{c}^\dagger) + \sqrt{2\kappa}\delta a_{fb}^{in}, \quad (19a)$$

$$\dot{\delta\hat{c}} = -(i\omega_c + \gamma_c)\delta\hat{c} + ig(\delta\hat{a} + \delta\hat{a}^\dagger) + \sqrt{2\gamma}\delta c^{in}, \quad (19b)$$

where g is defined as $g_0|\hat{a}_s|$, representing the light-enhanced optomechanical coupling. From comparing Eq. (19) and Eq. (7), it is evident that the harmonic oscillator in contact with the thermal bath corresponds to the cavity-field fluctuation (with effective frequency $\Omega_a = \Delta$ and damping rate κ_{fb}), while the harmonic oscillator in contact with the thermal bath corresponds to the mechanical mode fluctuation (with frequency $\omega_c = \omega_m$ and damping rate $\gamma_c = \kappa_c$).

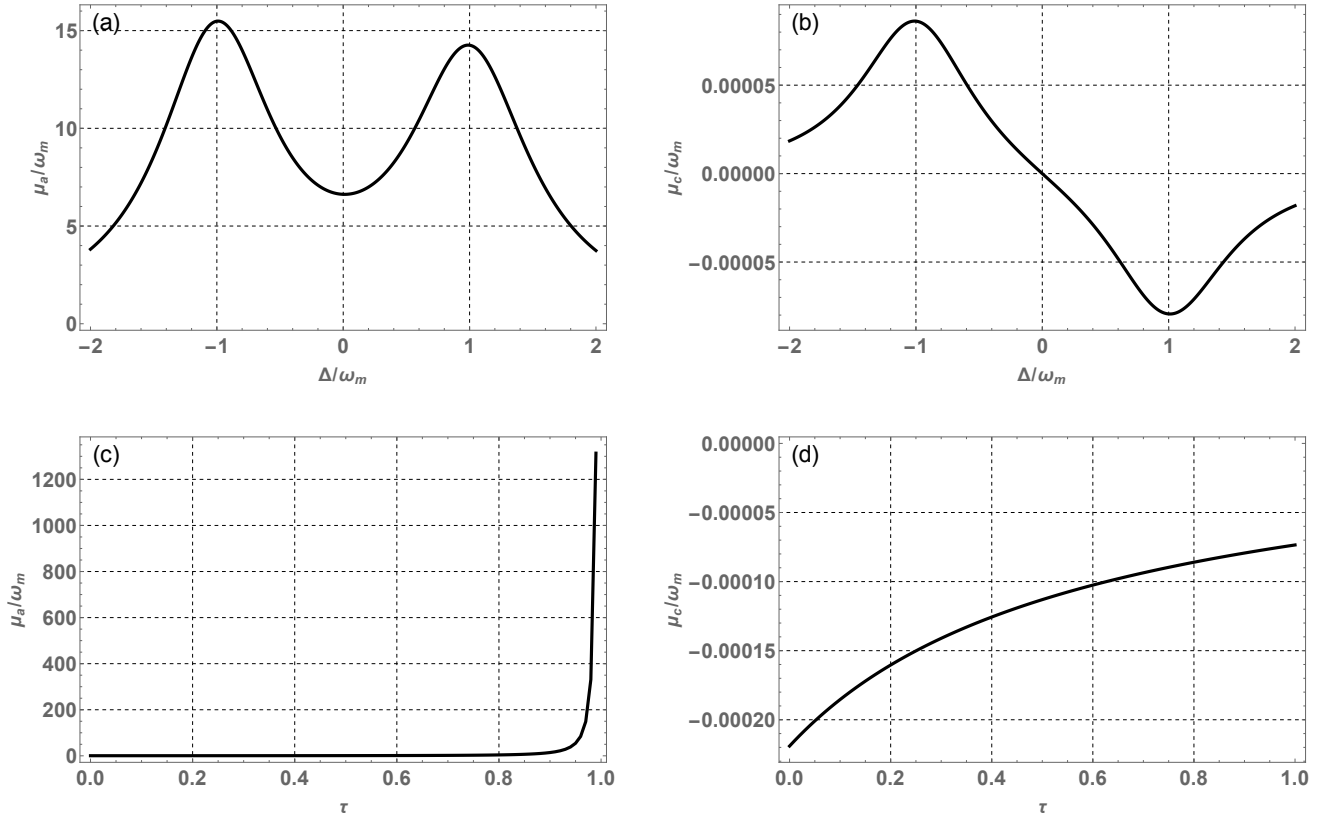


FIG. 8: Plot of the optical and mechanical contributions to the entropy production μ_a/ω_m and μ_c/ω_m as a function of normalized photon detuning Δ/ω_m with $\tau = 0.9$ (a)-(b), and of the reflectivity parameter τ with $\Delta = \omega_m$ (c)-(d). Other parameters $\kappa_a = 0.2\omega_m$, $\kappa_c = 10^{-3}\omega_m$, $g = 0.005\omega_m$, $N_a = 0$ and $N_c = 10^3$. With $\theta = \pi$.

The behavior of the optical (μ_a) and mechanical (μ_c) contributions to the entropy production against the normalized detuning is displayed in Fig. 8(a)-(b) for the case of coherent feedback. These plots reveal that for small coupling, the system is stable even in the blue-detuned region ($\Delta < 0$). Large detuning ($|\Delta| \gg 1$) effectively decouples the two oscillators, causing each to equilibrate with its bath, which results in vanishing Π_s . We observe that the contributions μ_a and μ_c to the entropy production peak at $\Delta = \pm\omega_m$. The peaks in the rate of entropy production at $\Delta > 0$ and $\Delta < 0$ demonstrate that the cooling and heating processes associated with these detuning regimes behave distinctly. This is shown by the entropy production rate's behavior, with clear peaks in both the optical (μ_a) and mechanical (μ_c) contributions at the two mechanical sidebands. For $\Delta \approx \omega_m$, the dominant beam splitter interaction $\hat{H}_I \propto \delta\hat{a}^\dagger\delta\hat{c} + \delta\hat{a}\delta\hat{c}^\dagger$ causes enhanced heat transport and a necessary increase in entropy. In the amplification regime, the peak is observed to be even more pronounced, as seen in Fig. 8(a). In the regime $\Delta \approx -\omega_m$, the dominant two-mode squeezing interaction $\hat{H}_I \propto \delta\hat{a}^\dagger\delta\hat{c}^\dagger + \delta\hat{a}\delta\hat{c}$ results in exponential growth of oscillator energies and induces strong correlations between the two modes, yielding EPR-like entanglement in the infinite energy limit. Consequently, our analysis indicates that the entropy production must increase accordingly. Conversely, the sign change of μ_b in Fig. 8(b) clearly indicates the mechanical resonator's heating/cooling. The behavior of Π_s and its contributions thus provides a full thermodynamical account of both the amplification and cooling regimes.

The optical (μ_a) and mechanical (μ_c) contributions to the entropy production are plotted as a function of the reflective parameter τ in Fig. 8(c)-(d). These figures reveal a significant enhancement of entropy production through coherent feedback. By re-injecting photons into the cavity, coherent feedback enhances the interaction between the optical and mechanical modes.

Fig. 9(a) and (b) present a comparison between the entropy production rate Π_s and the mutual information \mathcal{I} , which quantifies the correlations established by the optomechanical interaction. It can be seen that for small thermal phonon excitation ($N_c = 10$), Fig. 9(a) and (b) reveal that Π_s and \mathcal{I} are nearly identical across the entire range of detunings Δ . This indicates that the degree of irreversibility induced by the stationary process is directly related to the amount of shared correlations. In addition, Π_s and

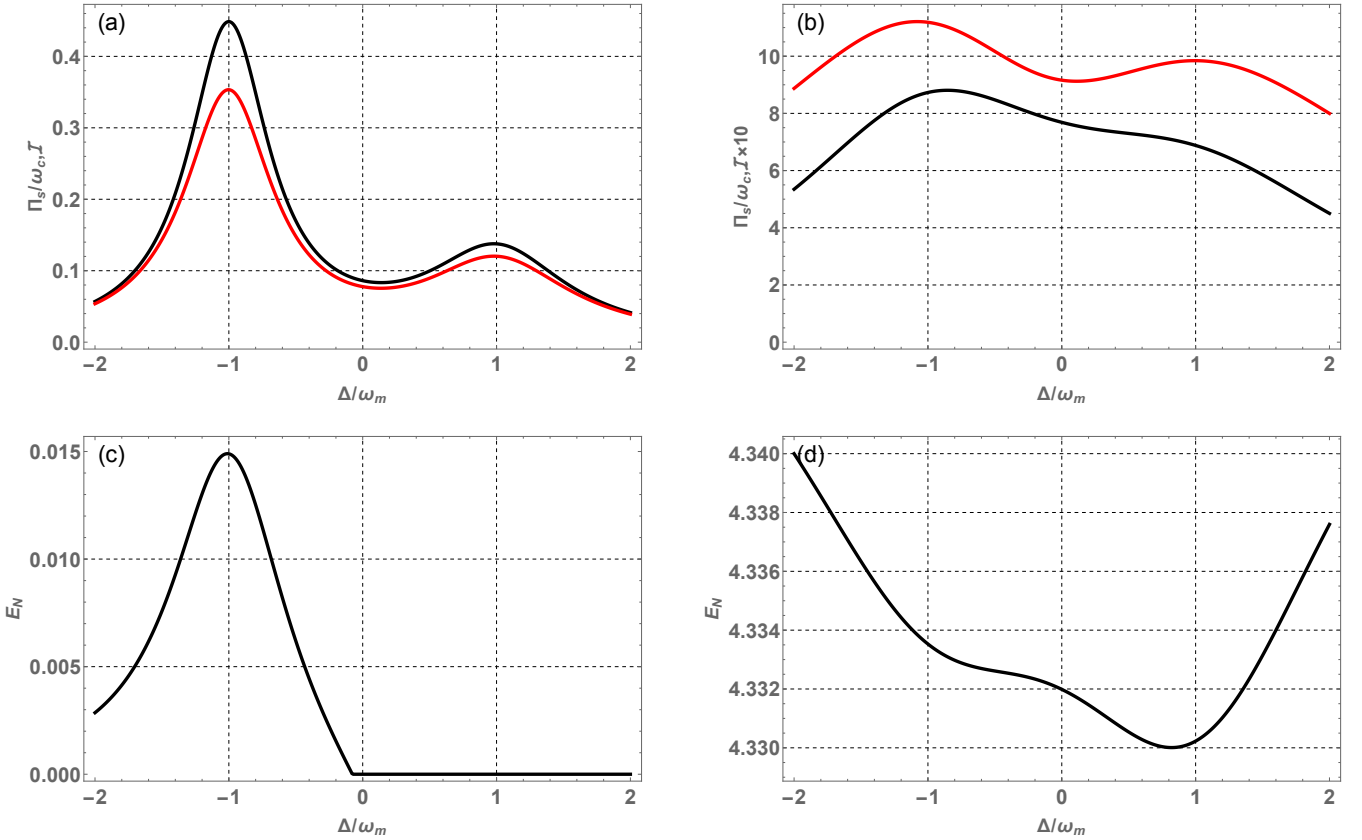


FIG. 9: Plot of the optical and mechanical contributions to the entropy production μ_a/ω_m and μ_c/ω_m as a function of normalized photon detuning Δ/ω_m with $\tau = 0$ in (a) and (c); and $\tau = 0.9$ in (b) and (d). Other parameters $\kappa_a = 0.5\omega_m$, $\kappa_c = 10^{-2}\omega_m$, $g = 0.05\omega_m$, $G = 2g$, $N_a = 0$ and $N_c = 10$. With $\theta = \pi$.

\mathcal{I} exhibit strong peaks around $\Delta = -\omega_m$. This is attributable to the strong quantum correlations (entanglement) established between the optical and mechanical modes, evident from Fig. 9(a). Increasing the reflective parameter τ leads to an increase in the entropy production rate Π_s , mutual information \mathcal{I} , and entanglement E_N , as demonstrated in Fig. 9(b) and (d).

VI. CONCLUSION

In summary, we have investigated the enhancement of the entropy production rate through the coherent feedback loop in a cavity optomechanical system where an optical cavity mode is coupled with movable mirror via radiation pressure. We have shown that in the small-coupling limit, the entropy production rate is proportional to the quantum mutual information. We use for application the optomechanical system of Fabry-Pérot type cavity, and show that the picks of the entropy production corresponding of the heating/cooling of movable mirror are improved. Therefore, we conclude that irreversibility and quantum correlations are not independent and must be analyzed jointly and could be enhanced via feedback control.

APPENDIX : Stationary entropy production rate

Explicit expressions for the entropy production rate $\Pi(t)$ and the entropy flux $\Phi(t)$ from Eq. (3) are provided in this Appendix, following the approach of Refs. [47–49]. The system's dynamics are described by the quantum Langevin equations for the vector $\hat{u} = (\hat{X}_a, \hat{Y}_a, \hat{X}_c, \hat{Y}_c)^T$. The relationship between the Wigner entropy and the covariance matrix (\mathcal{V}) for a Gaussian system is given by:

$$\mathcal{W}(u) = \frac{1}{\pi^n \sqrt{\det \mathcal{V}}} e^{-\frac{1}{2} u^T \mathcal{V}^{-1} u}, \quad (20)$$

This property of being always positive allows us to identify the Wigner function as a quasi-probability distribution in phase space (n is the number of bosonic modes). It provides a fully equivalent description of the density matrix. According to Ref. [53], the Wigner entropy is related to the Rényi-2 entropy and satisfies the strong subadditivity inequality. In recent years, the link between general Rényi- α entropies and the thermodynamic properties of quantum systems has also been a subject of interest [54, 55]. An equivalent description of the system's dynamics is given by the Fokker-Planck equation for the Wigner function $\mathcal{W}(u, t)$ (Eq. (20))

$$\frac{d\mathcal{W}}{dt} + \frac{d\mathbf{J}(u, t)}{du} = 0, \quad (21)$$

where $\hat{u} = (\hat{X}_a, \hat{Y}_a, \hat{X}_c, \hat{Y}_c)^T$ is a point in the phase space. The probability current vector is then defined as

$$\mathbf{J}(u, t) = \mathcal{A}u\mathcal{W}(u, t) - \frac{\mathcal{D}}{2} \frac{d\mathcal{W}(u, t)}{du}. \quad (22)$$

the drift matrix \mathcal{A} and the diffusion matrix \mathcal{W} defined in Eq. (11). Using the time-reversal operator $E = \text{diag}(1, -1, 1, -1)$, the dynamical variables are split according to their symmetry. Accordingly, the drift matrix \mathcal{A} is decomposed into an irreversible component \mathcal{A}^{irr} and a reversible component \mathcal{A}^{rev} ($\mathcal{A} = \mathcal{A}^{\text{rev}} + \mathcal{A}^{\text{irr}}$), where the irreversible component \mathcal{A}^{irr} is odd under time reversal [60]. Using the time-reversal operator, the irreversible component \mathcal{A}^{irr} and the reversible component \mathcal{A}^{rev} are constructed via $\mathcal{A}^{\text{irr}} = [\mathcal{A} + E\mathcal{A}E^T]/2$ and $\mathcal{A}^{\text{rev}} = [\mathcal{A} - E\mathcal{A}E^T]/2$. Their explicit forms are as follows

$$\mathcal{A}^{\text{rev}} = \begin{pmatrix} 0 & \Omega_{\text{fb}} & 0 & 0 \\ -\Omega_{\text{fb}} & 0 & G & 0 \\ 0 & 0 & 0 & \Omega_c \\ G & 0 & -\Omega_c & 0 \end{pmatrix} \quad \text{and} \quad \mathcal{A}^{\text{irr}} = \text{diag}(-\kappa_{\text{fb}}, -\kappa_{\text{fb}}, -\kappa_c, -\kappa_c). \quad (23)$$

While the diffusion matrix \mathcal{D} is purely irreversible ($\mathcal{D}^{\text{rev}} = 0$, so $\mathcal{D} \equiv \mathcal{D}^{\text{irr}}$), this separation induces a similar splitting in the probability current $\mathbf{J}(u, t) = \mathbf{J}_{\text{rev}}(u, t) + \mathbf{J}_{\text{irr}}(u, t)$, where:

$$\mathbf{J}^{\text{rev}}(u, t) = \mathcal{A}^{\text{rev}}u\mathcal{W}(u, t), \quad \text{and} \quad \mathbf{J}^{\text{irr}}(u, t) = \mathcal{A}^{\text{irr}}u\mathcal{W}(u, t) - \frac{\mathcal{D}}{2} \frac{d\mathcal{W}(u, t)}{du}. \quad (24)$$

The reversible part of the probability current is divergence-less ($\nabla_u \cdot \mathbf{J}_{\text{rev}}(u, t) = 0$), which can be seen from the form of Eq. (24). Substituting Eq. (24) into the expression for the entropy rate yields [42]

$$\frac{dS}{dt} = -\frac{1}{4} \int \left(\frac{d\mathcal{W}(u, t)}{dt} \right) \log \mathcal{W}(u, t) du. \quad (25)$$

The entropy rate can be expressed as, using Eqs. (21) and (25) and integrating by parts

$$\frac{dS}{dt} = -\frac{1}{4} \int du \{ \mathbf{J}^{\text{irr}}(u, t) \}^T \frac{1}{\mathcal{W}(u, t)} \frac{d\mathcal{W}(u, t)}{du}. \quad (26)$$

Substitution of Eq. (24) yields the splitting shown in Eq. (3) between entropy flux

$$\Phi(t) = -\frac{1}{4} \int du 2\mathbf{J}^{\text{irr}}(u, t)^T \mathcal{D}^{-1} \mathbf{J}^{\text{irr}}(u, t), \quad (27)$$

and entropy production rate

$$\Pi(t) = \frac{1}{4} \int du \frac{2}{\mathcal{W}(u, t)} \mathbf{J}^{\text{irr}}(u, t)^T \mathcal{D}^{-1} \mathbf{J}^{\text{irr}}(u, t). \quad (28)$$

The expression in Eq. 28 is identified with the entropy production rate due to its non-negativity, since Eq. (28) represents the integral of a quadratic form. For a Gaussian state, the relation $\{\frac{d\mathcal{W}}{du}\}\mathcal{V}(u, t) = -\mathcal{W}_V(u, t)\mathcal{V}^{-1}(t)u$ holds, which yields the irreversible component of the probability current as $\mathbf{J}^{\text{irr}}(u, t) = \mathcal{W}_V(u, t)[\mathcal{A}^{\text{irr}} + \mathcal{D}\mathcal{V}^{-1}(t)]u$. In the stationary state, the entropy production rate equals the negative of the entropy flux ($\Pi_s = -\Phi_s$), whose expression is [42]

$$\Pi_s = \text{tr}\{\mathcal{A}^{\text{irr}}\} + 2\text{tr}\{(\mathcal{A}^{\text{irr}})^T \mathcal{D}^{-1} \mathcal{A}^{\text{irr}} \mathcal{V}_s\}. \quad (29)$$

Π_s can be given in matrix form as

$$\Pi_s = 2\kappa_a \left(\frac{[\mathcal{V}_s]_{11} + [\mathcal{V}_s]_{22}}{2N_a + 1} - 1 \right) + 2\kappa_c \left(\frac{[\mathcal{V}]_{33} + [\mathcal{V}_s]_{44}}{2N_c + 1} - 1 \right). \quad (30)$$

[1] J. P. Sethna, *Entropy, Order Parameters, and Complexity* (Oxford University Press, Oxford, 2011).

[2] M. W. Zemansky, *Heat and Thermodynamics* (McGrawHill Book Company Inc., New York, 1968).

[3] U. Seifert, *Rep. Prog. Phys.* **75**, 126001 (2012).

[4] C. Jarzynski, *Annu. Rev. Condens. Matter Phys.* **2**, 329 (2011).

[5] I. Prigogine, *Introduction to thermodynamics of irreversible processes*, (John Wiley - Sons, 1968).

[6] L. Onsager, *Phys. Rev.* **37**, 405(1931).

[7] S. Machlup and L. Onsager, *Phys. Rev.* **91**, 1512(1953).

[8] J. Schnakenberg, *Rev. Mod. Phys.* **48**, 571(1976).

[9] T. Tom'e and M. J. de Oliveira, *Phys. Rev. E* **82**, 021120(2010).

[10] T. Tom'e and M. J. de Oliveira, *Phys. Rev. Lett.* **108**, 020601(2012).

[11] G. Lindblad, *Math. Phys.* **48**, 119 (1976).

[12] B. Leggio, A. Napoli, A. Messina, and H.-P. Breuer, *Phys. Rev. A* **88**, 042111(2013).

[13] C. O. Edet, M. Asjad, D. Dutykh, N. Ali and O. Abah, *Physical Review Research*, **6**(3), 033037 (2024).

[14] S. Shahidani, *Phys. Rev. A* **110**, 052216 (2024).

[15] J. P. Santos, G. T. Landi, and M. Paternostro, *Phys. Rev. Lett.* **118**, 220601 (2017).

[16] W. T. B. Malouf, J. P. Santos, L. A. Correa, M. Paternostro, and G. T. Landi, *Phys. Rev. A*, **99**, 052104(2019).

[17] S. Giordano, *Phys. Rev. E* **103**, 052116 (2021).

[18] J. P. Santos, L. C. Celeri, F. Brito, G. T. Landi, and M. Paternostro, *Phys. Rev. A* **97**, 052123 (2018). J. P. Santos, A. L. de Paula, R. Drumond, G. T. Landi, and M. Paternostro, *Phys. Rev. A* **97**, 050101(R) (2018).

[19] M. Huber, *et al.* *New J. Phys.* **17**, 065008 (2015).

[20] M. Brunelli, L. Fusco, R. Landig, W. Wieczorek, J. HoelscherObermaier, G. Landi, F. L. Semiao, A. Ferraro, N. Kiesel, T. Donner, G. De Chiara, and M. Paternostro, *Phys. Rev. Lett.* **121**, 160604 (2018).

[21] H. M. Wiseman, G.J. Milburn, *Phys. Rev. Lett.* **70**, 548 (1993). *PhysRevLett.70.548*

[22] H. M. Wiseman, G.J. Milburn, *Phys. Rev. A* **47**, 642 (1993).

[23] S. Mancini, D. Vitali, P. Tombesi, *Phys. Rev. Lett.* **80**, 688 (1998).

[24] J.-M. Courty, A. Heidmann, M. Pinard, *Eur. Phys. J. D* **17**, 399 (2001).

[25] D. Vitali, S. Mancini, L. Ribichini, P. Tombesi, *Phys. Rev. A* **65**, 063803 (2002).

[26] D. Ristè, M. Dukalski, C.A. Watson, G. de Lange, M.J. Tiggelman, Y.M. Blanter, K.W. Lehnert, R.N. Schouten, L. DiCarlo, *Nature* **502**, 350 (2013).

[27] M. Rossi, N. Kralj, S. Zippilli, R. Natali, A. Borrielli, G. Pandraud, E. Serra, G. Di Giuseppe, D. Vitali, *Phys. Rev. Lett.* **119**, 123603 (2017).

[28] N. Kralj, M. Rossi, S. Zippilli, R. Natali, A. Borrielli, G. Pandraud, E. Serra, G.D. Giuseppe, D. Vitali, *Quantum Sci. Technol.* **2**, 034014 (2017).

[29] P. Bushev, D. Rotter, A. Wilson, F.M.C. Dubin, C. Becher, J. Eschner, R. Blatt, V. Steixner, P. Rabl, P. Zoller, *Phys. Rev. Lett.* **96**, 043003 (2006).

[30] M. Koch, C. Sames, A. Kubanek, M. Apel, M. Balbach, A. Ourjoumtsev, P.W.H. Pinkse, G. Rempe, *Phys. Rev. Lett.* **105**, 173003 (2010).

[31] J. Gieseler, B. Deutscher, R. Quidant, L. Novotny, *Phys. Rev. Lett.* **109**, 103603 (2012).

[32] M.G. Genoni, J. Zhang, J. Millen, P.F. Barker, A. Serafini, *New J. Phys.* **17**, 073019 (2015)

[33] D.F. Walls, G.J. Milburn, *Cavity modes*, in: *Quantum Optics*, Springer, Berlin, Germany, 1998, pp. 121–124.

[34] J. Li, G. Li, S. Zippilli, D. Vitali, T. Zhang, *Phys. Rev. A* **95**, 043819 (2017).

[35] S. Huang, A. Chen, *Appl. Sci.* **9** (16) (2019) 3402.

[36] A. Harwood, M. Brunelli, and A. Serafini, *Physical Review A*, **103**(2), (2021) 023509.

[37] M. Ernzer, M. Bosch Aguilera, M. Brunelli, G. L. Schmid, T. M. Karg, C. Bruder and P. Treutlein, *Physical Review X*, **13**(2) (2023) 021023.

[38] M. Amazioug, B. Maroufi, M. Daoud, *Phys. Lett. A* **384**, 126705 (2020).

[39] L. Henderson, V. Vedral, *J. Phys. A* **34** (35), 6899 (2001).

[40] K. Modi, A. Brodutch, H. Cable, T. Paterek and V. Vedral, *Rev. Mod. Phys.* **84**, 1655 (2012).

[41] M. Aspelmeyer, T. Kippenberg, and F. Marquardt, *Rev. Mod. Phys.* **86**, 1391 (2014).

[42] M. Brunelli and M. Paternostro, *Irreversibility and correlations in coupled quantum oscillators*, arXiv preprint arXiv:1610.01172 (2016).

[43] A. Asadian, D. Manzano, M. Tiersch, and H. J. Briegel, *Phys. Rev. E* **87**, 012109 (2013).

[44] M. Ernzer, M. Bosch Aguilera, M. Brunelli, et al. *Physical Review X*, 2023, vol. 13, no 2, p. 021023.

[45] A. Harwood, M. Brunelli and A. Serafini, *Physical Review A*, **103**(2), 023509 (2021).

[46] A. Serafini, *Quantum Continuous Variables* (CRC Press, 2017).

[47] G. T. Landi, T. Tome, and M. J. de Oliveira, *Entropy production in linear Langevin systems*, *J. Phys. A Math. Theor.* **46**, 395001(2013).

[48] M. Brunelli, M. Paternostro, *Irreversibility and correlations in coupled quantum oscillators*, arXiv:1610.01172.

[49] M. Brunelli, L. Fusco, R. Landig, W. Wieczorek, J. Hoelscher-Obermaier, G. Landi, F. L. Semiao, A. Ferraro, N. Kiesel, T. Donner, G. De Chiara, and M. Paternostro, *Phys. Rev. Lett.* **121**, 160604 (2018).

[50] W. T. B. Malouf, J. P. Santos, L. A. Correa, M. Paternostro, and G. T. Landi, *Phys. Rev. A*, **99**, 052104 (2019).

[51] D. S. P. Salazar and G.T. Landi, *Phys. Rev. Research* **2**, 033090 (2020).

[52] V. Vedral, *Rev. Mod. Phys.* **74**, 197 (2002).

[53] G. Adesso, D. Girolami, and A. Serafini, *Phys. Rev. Lett.* **109**, 190502 (2012).

- [54] B.-B. Wei and M. B. Plenio, Relations between Dissipated Work and Renyi Divergences, *New J. Phys.* 19, 023002(2017).
- [55] F. G. S. L. Brandao, M. Horodecki, N. H. Y. Ng, J. Oppenheim, and S. Wehner, The second laws of quantum thermodynamics, *Proc. Natl. Acad. Sci. U.S.A.* 112, 3275 (2015).
- [56] M. B. Plenio, *Phys. Rev. Lett.* 95, 090503 (2005).
- [57] G. Vidal, R.F. Werner, *Phys. Rev. A* 65, 032314 (2002).
- [58] G. Adesso, A. Serafini, F. Illuminati, *Phys. Rev. A* 70, 022318 (2004).
- [59] L. Mandel, E. Wolf, Effect of an attenuator or beam splitter on the quantum field, in: *Optical Coherence and Quantum Optics*, Cambridge University Press, Cambridge, UK, 1995, pp. 639–640.
- [60] R. E. Spinney and I. J. Ford, *Phys. Rev. E* 85, 051113 (2012).
- [61] D. Vitali, et al. *Physical review letters* 98.3, 030405 (2007).
- [62] M. Asjad, P. Tombesi and D. Vitali. *Physical Review A*, 94(5), 052312 (2016).
- [63] J. Zhang et al., *Phys. Rev. A* 68, 013808 (2003).
- [64] M. Pinard et al., *Europhys. Lett.* 72, 747 (2005).
- [65] D. F. Walls and G. J. Milburn, *Quantum Optics* (Springer, Berlin, 1994).